Accurate Diffusion Coefficients of Organosoluble Reference Dyes in Organic Media Measured by Dual-Focus Fluorescence Correlation Spectroscopy

Karel Goossens,[†,‡] Mira Prior,[§] Victor Pacheco,[⊥,∥] Dieter Willbold,[⊥,#] Klaus Müllen,[▽] Jörg Enderlein,[§] Johan Hofkens,[†] and Ingo Gregor*[,§]

[†]KU Leuven, Department of Chemistry, Celestijnenlaan 200F (PO Box 2404), 3001 Heverlee, Belgium, [‡]Center for Multidimensional Carbon Materials, Institute for Basic Science (IBS), 101-dong, UNIST-gil 50, Eonyang-eup, Ulju-gun, Ulsan 689-798, Republic of Korea, [§]Georg August University, Third Institute of Physics, Friedrich-Hund-Platz 1, 37077 Göttingen, Germany, [⊥]Research Centre Jülich, Institute of Complex Systems: Structural Biochemistry (ICS-6), Wilhelm-Johnen-Straße, 52425 Jülich, Germany, [∥]Albert Ludwigs University, Institute for Macromolecular Chemistry, Hermann-Staudinger-Haus, Stefan-Meier-Straße 31, 79104 Freiburg, Germany, [#]Heinrich Heine University, Institute for Physical Biology, Universitätsstraße 1, 40225 Düsseldorf, Germany, and [▽]Max Planck Institute for Polymer Research, Ackermannweg 10, 55128 Mainz, Germany

ABSTRACT Dual-focus fluorescence correlation spectroscopy (2fFCS) is a versatile method to determine accurate diffusion coefficients of fluorescent species in an absolute, reference-free manner. Whereas (either classical or dual-focus) FCS has been employed primarily in the life sciences and thus in aqueous environments, it is increasingly being used in materials chemistry, as well. These measurements are often performed in nonaqueous media such as organic solvents. However, the diffusion coefficients of reference dyes in organic solvents are not readily available. For this reason we determined the translational diffusion coefficients of several commercially available organosoluble fluorescent dyes by means of 2fFCS. The selected dyes and organic solvents span the visible spectrum and a broad range of refractive indices, respectively. The diffusion coefficients can be used as absolute reference values for the calibration of experimental FCS setups, allowing quantitative measurements to be performed. We show that reliable information about the hydrodynamic dimensions of the fluorescent species (including noncommercial compounds) within organic media can be extracted from the 2fFCS data.

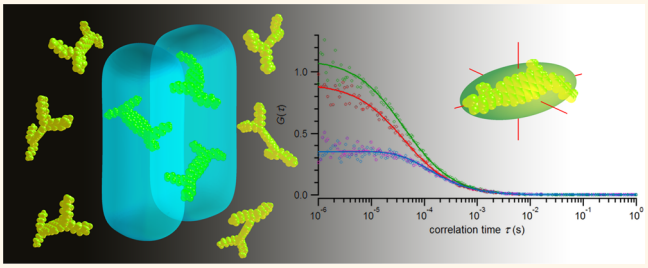

KEYWORDS: diffusion · fluorescence · organic media · calibration · dual-focus fluorescence correlation spectroscopy

Thermally induced ("Brownian") translational diffusion is one of the fundamental processes that occur in solution. The translational diffusion constant D_T of a particular (spherically shaped) solute allows calculating its (hydrodynamic) Stokes radius r_H and thus its size *via* the Stokes–Einstein relation eq 1.

$$r_H = \frac{k_B T}{6\pi\eta D_T} \quad (1)$$

where k_B is the Boltzmann constant, T is the sample temperature, and η is the viscosity of the solution.

Any change in the Stokes radius of a fluorescent reporter molecule will be directly reflected in its translational diffusion constant. Such a change can originate, for instance, from binding of a fluorescent solute molecule to a catalyst particle. On the other hand, changes in the viscosity of the sample mixture, for example in the course of a polymerization reaction, will also result in changes of the translational diffusion constant.[1] It is clear that a precise and accurate measurement of diffusion constants is of utmost importance, especially when only small changes in Stokes radius (in the range of a few Ångstrøm) need to be examined. Conveniently, the diffusion is measured by a fluorescence-based experimental technique such as fluorescence correlation spectroscopy (FCS) or wide-field microscopy single-particle tracking (SPT). The former technique allows to investigate fast

* Address correspondence to ingo.gregor@phys.uni-goettingen.de.

Received for review April 20, 2015 and accepted July 4, 2015.

Published online July 04, 2015
10.1021/acsnano.5b02371

moving dyes in environments of relatively low viscosity, while the latter technique enables one to monitor slowly diffusing probe molecules.[2,3] Besides the fluorescence-based single-molecule measurements other methods for accurate diffusion constant determination include dynamic light scattering (DLS), pulsed-field gradient nuclear magnetic resonance spectroscopy (pfgNMR), Taylor dispersion analysis, plug broadening in capillary flow or electrophoresis, and analytical ultracentrifugation. However, these methods require much higher sample concentrations than those commonly used in FCS (from 1×10^{-8} M to 1×10^{-12} M). As a result, in order to obtain a correct estimation of the Stokes radius (in the infinite-dilution limit, where intermolecular interactions can be neglected), one usually has to measure at different concentrations and to extrapolate the concentration/diffusion constant curve toward zero concentration.[4−6] Moreover, the fact that many organosoluble dye molecules tend to aggregate in organic solvents renders the possibility of working at low sample concentrations even more attractive.

FCS was invented in the 1970s by Magde, Elson, and Webb.[7−10] In classical FCS the sample is excited by a tightly focused laser beam. A small pinhole in the detection path rejects fluorescence emitted out-of-focus defining a small confocal detection volume (usually on the order of one femtoliter or less). The fluorescence intensity emitted from molecules in the confocal volume is recorded and the underlying time-dependence of the signal is analyzed by means of the autocorrelation function (ACF). For a sufficiently small average number of fluorophores within the confocal volume, the fluorescence fluctuations are dominated by the random diffusion of the dye molecules, and the ACF shows a decay reflecting the average observation time of the molecules which is directly related to the diffusion constant. This is the simplest case, since nondiffusion-related phenomena—typically photophysical processes, such as excursions to the triplet state—can also cause a flickering in the fluorescence intensity and, hence, are rendered by the ACF. Usually, these processes happen much faster than the diffusion and, thus, do not affect the analysis of the diffusion process.

In order to deduce the diffusion constant from the measured diffusion time one needs to know the shape and size of the detection volume, or more precisely the so-called molecule detection function (MDF). This function describes the probability to excite and detect a fluorescence photon from a molecule at any position within the sample. Unfortunately, the exact shape of the MDF in a confocal microscopy setup depends on many imprecisely known parameters.[11,12] Usually, the MDF is approximated by a three-dimensional Gaussian profile, whose half axes can be determined by measuring the diffusion time of a reference dye with known diffusion constant (the experimental conditions during calibration—laser excitation wavelength and power, cover slide thickness, immersion medium, solvent, temperature, *etc.*—must be the same as during the actual measurements).[13] Although the assumption of a three-dimensional Gaussian MDF does not give a completely correct picture of the actual detection volume,[14−16] the calibration method with reference dyes became the standard approach and has proven its value for a long time.[17] For many water-soluble dyes there already exist standard reference data on their diffusion constant in aqueous solution at a particular temperature.[4,18−23] The known temperature dependence of the viscosity of water allows calculating a reference diffusion constant at different temperatures.

In 2007 we established the concept of "dual-focus" FCS (2fFCS).[4,18−20,24−32] This method introduces an intrinsic "ruler" into the measurement. We showed that this method, in contrast to classical FCS, is largely insensitive to cover slide thickness variations, refractive index mismatches, laser beam astigmatism (aberration), and—very importantly—optical saturation of the chromophores. A train of excitation laser pulses with temporally alternating orthogonal polarization is created, either (i) by using two identical, linearly polarized, alternately pulsed lasers whose beams are combined by a polarizing beam splitter;[4] or (ii) by using only one pulsed laser in combination with polarizing beam splitters and an optical fiber delay;[18] or (iii) by using a single continuous wave laser in combination with an electro-optical modulator.[19,33]

By inserting a Nomarski prism (normally used for differential interference contrast (DIC) microscopy) in the excitation path between the dichroic mirror and the objective lens, two laterally shifted but overlapping excitation foci are generated in the sample solution. The wavelength-dependent lateral distance between the foci, which is determined solely by the optical properties of the Nomarski prism, can be obtained from a calibration with monodisperse multifluorescent polymer beads of known size or from a calibration measurement of a dye with a known diffusion constant. The interfocal distance remains fixed despite possible optical aberrations or saturation effects that may distort the shape of the MDF of each focus.[4,11,12] In this way the distance can be used as a ruler for the diffusion constant determination.

Using "pulsed interleaved excitation" (PIE)[34,35] and time-correlated single-photon counting (TCSPC), one can assign each detected photon to the laser pulse that excited the molecule and thus to the corresponding focal volume. By determining the fluorescence intensity ACF for each focus separately as well as the cross-correlation function (CCF) between photons emerging from both foci, and analyzing the decay of the CCF in comparison to the ACF decay (which is due to the extra distance between both foci), it is possible to calculate the diffusion constant of the fluorescent molecules

absolutely and without a reference. We thus found that the diffusion constant of the widely used reference dye Rhodamine 6G is by 37% larger than the value used in most publications on FCS over the last three decades.[18]

Despite the potential of 2fFCS to determine absolute diffusion constants in a largely artifact-free way, classical FCS is still in widespread use. The technique is primarily used in the life sciences, for example to monitor interactions with antibodies,[36] protein−protein interactions,[37] or conformational changes in proteins upon ion binding or unfolding.[38] These experiments are performed in aqueous environments. As stated above, standard reference diffusion constants in aqueous solution are available for many water-soluble dyes. Nonetheless, FCS has also found its way to the chemical and materials science communities,[1−3,39−70] where measurements are often performed in nonaqueous environments, such as organic solvents or polymer solutions. However, no calibration data are readily available for the diffusion constants of organosoluble reference dye molecules. This prohibits a straightforward calibration of an experimental classical single-focus FCS setup and the ability to perform quantitative measurements.

Some calibration methods have been proposed previously. Zettl *et al.* suggested to use dye-labeled polymer chains of different molecular weights.[44,50,56,58] They synthesized multiple batches of polystyrene labeled with Rhodamine B, by means of (controlled) anionic polymerization and subsequent attachment of the dye to the polymer chain end. The polymer molecular weights ranged between $M_w = 1 \times 10^4$ g mol^{-1} and $M_w = 1 \times 10^6$ g mol^{-1}, while the polydispersity was $M_w/M_n \sim 1.05$. FCS measurements on the differently sized polymers in toluene ($c \approx 1 \times 10^{-8}$ M) resulted in a calibration curve of diffusion time *versus* molecular weight, which could be fitted with a straight line. The slope of this line yields the principal half axes (or "waist") of the confocal volume element, since the relationship between diffusion constant and molecular weight is known for the polystyrene/toluene system.

Liu *et al.* calibrated the confocal volume element by comparing the results of DLS measurements and FCS measurements on polystyrene ($M_w \approx 3.90 \times 10^5$ g mol^{-1}, $M_w/M_n < 1.10$) labeled with Rhodamine B.[46] The postpolymerization labeling procedure required three synthesis steps.

Similarly, Cherdhirankorn *et al.* prepared fluorescently labeled polystyrene of different molecular weights ($M_w \approx 3.4 \times 10^4$ g mol^{-1} to 34.0×10^4 g mol^{-1}) and narrow size distribution (M_w/M_n = 1.05 to 1.17) using a perylene-3,4-dicarboximide (PMI) derivative bearing a styrene group.[52−54] The diffusion constants of these polymers in toluene, tetrahydrofuran (THF), and acetophenone were determined independently using DLS, which allowed to calibrate the FCS confocal volume element. This procedure was also used in chloroform and *o*-dichlorobenzene.[59,66]

Koynov *et al.* measured the Stokes radius of commercially available, fluorescently labeled silica nanoparticles in DMSO by DLS, and used this value to calibrate their FCS setup.[49]

The drawbacks of the mentioned methods are obvious. Although a limited amount of fluorescently labeled polymers are commercially available, the macromolecules used hitherto for FCS calibration purposes were prepared by the authors themselves (either by dye copolymerization or postpolymerization labeling). Synthesis, purification and analysis of the polymer samples is time-consuming. Two conditions need to be met: (i) the polymers should be highly monodisperse, since a broad distribution of chain lengths will inevitably result in a distribution of diffusion constants and the inability to fit the experimental ACF with a simple model for free three-dimensional diffusion; (ii) the incorporated fluorophore should match the available laser excitation wavelength(s), which makes it even more difficult to find a suitable sample that can be acquired from a commercial supplier. Furthermore, depending on the molecular weight and the physical aggregation state, some polymers take quite some time to dissolve in a particular solvent. Most importantly, the use of fluorescently labeled polymers for FCS calibration requires multiple measurements. If one has access to DLS instrumentation, both the polymer diffusion constant and the polymer diffusion time need to be determined by means of DLS and FCS, respectively, before one can calibrate the FCS confocal volume element. The method proposed by Zettl *et al.* requires the availability and measurement of multiple polymer samples of different molecular weight, as well as knowledge of the relationship between diffusion constant and molecular weight for a particular polymer/solvent system. On the other hand, the use of fluorescently labeled nanoparticles (Koynov *et al.*) or quantum dots also requires additional DLS measurements, and the samples need to be highly monodisperse. It should be noted that, because of these reasons, some groups have calibrated their FCS setups with "classical" aqueous dye solutions.[1,45,47,48,51,57] However, this should be avoided because it results in incorrect diffusion constants and Stokes radii.

To circumvent the problems associated with the methods discussed above, and to allow a straightforward and fast calibration of a classical FCS setup, we have measured the translational diffusion constants of several commercially available, organosoluble low molecular weight fluorescent dyes in different organic solvents by means of 2fFCS. These accurate values can be used as absolute reference standards for FCS. As is the case for water, knowledge of the temperature dependence of the viscosity of the organic

solvent allows to calculate a reference diffusion constant at different temperatures.[71−74] Low molecular weight fluorescent molecules have the advantage of high purity and monodispersity (spectroscopic purity in the visible spectrum can be easily checked, for instance, by thin layer chromatography (TLC)), solubility in a range of organic solvents and a lower tendency for aggregation than high molecular weight species, and they are widely commercially available—often in fairly large amounts for a reasonable price.

RESULTS AND DISCUSSION

Translational Diffusion Constants and Stokes Radii. We determined the translational diffusion constants D_T of the selected dyes in the chosen solvents using 2fFCS. Typical 2fFCS correlation curves are shown illustratively in Figure 1 and in Figure S3 (see Supporting Information). The obtained diffusion constants were independent of excitation intensity (provided the laser excitation power is kept sufficiently low as to avoid photobleaching), in contrast to classical FCS measurements.[4,20,24] The D_T values as well as the corresponding Stokes radii r_H (calculated *via* eq 1) are listed in Table 1. The uncertainties of the obtained values are dominated by the precision of the experimental conditions. Most importantly, the distance of the two foci is known with a precision of 1% and the absolute temperature has an uncertainty of 1K. However, the statistical variance of the fitted parameters is in the order of 0.1%, only. We can present the values of the Stokes radius with an accuracy of 1 Å.

The diffusion constants and corresponding Stokes radii obtained by pfgNMR measurements are listed in Table 2. Table 3 shows the estimated molecular dimensions as obtained by molecular modeling. Also the Stokes radii that were computed from the obtained structures are listed.

Commercially Available Fluorescent Probes. We found that dye **1** is a suitable reference dye upon excitation with λ_{ex} = 470 nm laser light in all selected solvents (*i.e.*, ethanol, chloroform, THF, and toluene). Its Stokes radius was quite similar in all solvents. In chloroform r_H of **1** appeared to be smaller than in the other solvents, but the difference is still within the error margin of the experiment. This result was confirmed by pfgNMR (^{1}H DOSY) measurements on solutions of **1** in ethanol-d_6, $CDCl_3$, THF-d_8 and toluene-d_8 which find the very same Stokes radius for all solvents.

Just like dye **1**, compound **3** could also be used in all four solvents, in this case upon excitation with λ_{ex} = 531 nm laser light. The r_H values were again very similar, except in THF for which the Stokes radius appeared to be a little smaller. However, this also lies within the error margins. Systematically different values of the Stokes radius are obtained from pfgNMR measurements of this compound. The origin of this discrepancy is not clear. The obtained Stokes radii from the 2fFCS measurements correspond quite well to the theoretical dimensions of **3** (see Table 3). This might be a hint that the NMR measurements may show some bias. Compound **3** is a hydrophobic dye and it dissolved much slower in ethanol than in the

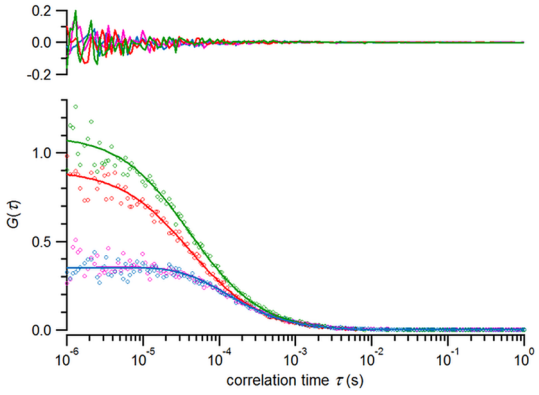

Figure 1. 2fFCS measurements of nanomolar solutions of 1 in chloroform. Average excitation power was 10 μW per laser. The normalized ACFs for the first focus (red) and second focus (green), and the forward CCF (blue) and reverse CCF (magenta) between both foci are shown. Circles are experimental values, solid lines are global fits using eq 6. Residuals are depicted above the graph.

TABLE 1. Translational Diffusion Constants of Organosoluble Reference Dyes in Selected Organic Solvents As Determined by 2fFCS, and Their Corresponding Stokes Radii As Calculated *via* eq 1

	excitation wavelength		diffusion constant at 294.15 K	Stokes radius
dye	λ_{ex}/nm	solvent	$D_T/\mu m^2\ s^{-1}$	r_H/nm
1	470	ethanol	318(10)	0.6(1)
		chloroform	838(10)	0.5(1)
		THF	771(46)	0.6(1)
		toluene	674(40)	0.6(1)
6	470	THF	522(10)	0.9(1)
		toluene	444(10)	0.8(1)
2	531	ethanol	345(10)	0.5(1)
3	531	ethanol	162(5)	1.1(1)
		chloroform	333(10)	1.1(1)
		THF	425(10)	1.0(1)
		toluene	334(10)	1.1(1)
7a	531	THF	326(14)	1.4(1)
		toluene	280(15)	1.3(1)
7b	531	THF	219(10)	2.0(1)
		toluene	174(5)	2.1(1)
7c	531	THF	145(5)	3.1(1)
		toluene	123(5)	3.0(1)
9a	531	toluene	100(2)	3.7(1)
9b	531	toluene	63(1)	6.0(1)
4	635	ethanol	419(10)	0.4(1)
5	635	chloroform	608(14)	0.6(1)
		THF	726(29)	0.6(1)
		toluene	630(18)	0.6(1)
8	635	THF	428(10)	1.0(1)
		toluene	349(10)	1.1(1)

TABLE 2. Translational Diffusion Constants of Organosoluble Reference Dyes in Selected Organic Solvents As Determined by pfgNMR, and Their Corresponding Stokes Radii As Calculated *via* eq 1

		diffusion constant at 298.15 K	Stokes radius
dye	solvent	$D_T/\mu m^2\ s^{-1}$	r_H/nm
1	ethanol-d_6	347(15)	0.5(1)
	$CDCl_3$	670(30)	0.6(1)
	THF-d_8	692(36)	0.6(1)
	toluene-d_8	597(35)	0.6(1)
2	ethanol-d_6	319(15)	0.6(1)
3	$CDCl_3$	533(25)	0.8(1)
	THF-d_8	520(25)	0.8(1)
	toluene-d_8	487(25)	0.7(1)

TABLE 3. Extensions along the Principal Axes of Rotation of the Investigated Organosoluble Reference Dyes, As Obtained by Molecular Modeling[a]

dye	Stokes radius	shape factor		Ψ	Θ	Φ	spheroid dimensions	
	r_H / nm	f_S / nm		p / nm	q / nm	r / nm	a / nm	b / nm
1	0.6			0.4	0.9	1.5		
2	0.6			0.4	0.9	1.5		
3	1.1	0.9	1.1	0.9	2.2	2.5	0.9	2.4
4	0.6			0.4	0.7	1.4		
5	0.9	0.7	0.9	0.8	1.2	2.2	2.2	1.0
6	1.0	0.9	1.2	0.8	1.5	2.8	2.8	1.2
7a	1.3	1.4	2.0	2.2	3.0	3.2	2.2	3.1
7b	1.9	1.7	2.3	2.2	3.6	4.1	2.2	3.9
7c	2.5	2.3	3.3	3.7	4.7	5.4	3.7	5.1
8	1.2	1.1	1.5	1.4	2.4	2.9	1.4	2.7
9a	3.0	2.9	4.3	5.5	6.2	5.6	6.2	5.6
9b	5.1	5.4	8.1	10.5	10.3	11.6	11.6	10.4

[a] Geometry optimization with MOPAC2012,[76] using the semiempirical PM7 Hamiltonian (**1**—**6**, and **8**) or by means of molecular mechanics in Chem3D Ultra, using the MM2 parameter set and force field (**7a**—**7c**, **9a**, and **9b**). The Stokes radii were estimated using Hydropro10.[77] The shape factors were calculated using eqs 3 and 4. Left numbers are valid for *stick* boundary conditions, right numbers are corrected for *slip* boundary conditions.

less polar solvents. The limited solubility prevents NMR measurements of this dye in ethanol. However, the 2fFCS measurements of **3** in ethanol gave very satisfactory results and no indications for aggregation could be found. In order to provide a better suited commercially available alternative in this spectral range, we determined the translational diffusion constant of dye **2** in ethanol. For this dye, 2fFCS and pfgNMR revealed the same Stokes radius as for compound **1**. The similarity of the chemical structure of the dyes **1** and **2** indicates that this result was to be expected.

The good agreement between the 2fFCS and pfgNMR results can be seen as a validation of the 2fFCS data, confirming that 2fFCS is a rapid, sensitive, precise and low-consumption tool for the accurate quantitative determination of diffusion properties within small sample volumes.

Compound **4** is a red-fluorescing probe that is best suited for more polar solvents like ethanol. Dye **5** is the better choice for apolar solvents. It showed very similar Stokes radii in chloroform, THF and toluene. Although this dye visually dissolved easily in ethanol, the obtained correlation functions could not be easily fitted. Even the incorporation of two triplet state ('dark state') relaxation times in the fitting functions did not yield satisfactory results. This indicates that in polar solvents the highly apolar octadecyl chains cause unwanted effects, such as interactions with the chromophore, micelle formation, or other.

The dimensions of the molecules as derived from the 2fFCS experiments and the estimations of the Stokes radii obtained from molecular modeling agree pretty well for the compounds **1**—**3**. For compounds **4** and **5** the modeling predicts Stokes radii that are too large. The molecular structure of **5** contains two flexible octadecyl residues. The structure found by the modeling represents just a temporal snapshot of the solution structure, making it difficult to predict a valid Stokes radius. Additionally, compounds **4** and **5** are salts and the optimization was done for the cations, only. Since a dissociation of the salts in organic solvents is unlikely, the influence of the associated anion on the structure is hard to predict. This might also explain the observed discrepancies.

PDI and TDI Fluorescent Probes. We also measured solutions of the noncommercial dyes **6**, **7a**, **7b**, **7c**, and **8** in the apolar solvents THF and toluene. For all compounds the obtained Stokes radii agree well in both solvents. The multichromophoric compounds **9a** and **9b** could be measured in toluene only.

The smallest dye in this series, compound **6**, shows a slightly smaller Stokes radius than it was predicted by the theoretical model. Because of the four heptyl chains linked to the chromophore, the same arguments hold for this compound as for compound **5**.

Compound **8** shows the same "bay" substituents as compound **7a** but bears a terrylenediimide instead of a perylenediimide core. At first sight one would expect a small increase of the Stokes radius from **7a** to **8**. However, we see a decrease from $r_H \approx 1.3$ nm to $r_H \approx 1.1$ nm. Also the theoretical modeling predicts a small decrease. In the terrylene compound **8**, the distance between the 4-[(2,3,4,5-tetraphenyl)phenyl]phenoxy substituents in the "bay" positions of the rylene core is larger than in its perylene analogue **7a**. One may reason that this allows greater rotational freedom for the substituents. As such, one may expect, in the same way as for **5**, to measure a slightly smaller value than expected. The higher flexibility may also reduce the impact of friction by the solvent, which also could result in a smaller effective Stokes radius.

Dyes **7a**, **7b** and **7c** are increasingly larger analogues of compound **3**, but due to the perylene core and the polyphenylene backbones they still have a rigid ("shape-persistent") structure that does not collapse onto itself.[75] The available computer power did not allow optimizing the structures of compounds **7a**, **7b**, and **7c** as well as of compounds **9a** and **9b** using the same semiempirical Hamiltonian as for the smaller compounds. Therefore, we had to model the structures using the simple force field MM2. We find a systematically increasing deviation of the estimated Stokes radius from the experimental values. Whereas for compound **7a** both values agree, we find a difference of −7% for **7b**, −19% for **7c**, −19% for **9a**, and −15% for **9b**. The experimental Stokes radii are consistently larger than the theoretical values indicating that the model implied in eq 1—the diffusing object is a hard sphere with radius r_H—does not describe the real structures of the molecules in solution with the required precision. This will be further discussed in the next section.

Extensions to the Stokes−Einstein Relation. The correspondence between modeling and experimental Stokes radii of the large compounds **7b**, **7c**, **9a**, and **9b** was rather unsatisfactory. Given the fact that the accuracy of the optimization of these structures was limited by computational constraints, one can reason that a computation of r_H based on a detailed structural model (as used by Hydropro10) will be accordingly inaccurate. A different approach is to directly account for the average shape of the molecule in the friction coefficient (*i.e.*, the denominator in eq 1). This should be less dependent on the structural details of the molecule. Modifications of the friction coefficient have been reported to describe the diffusion of nonspherical molecules, such as prolate spheroids, oblate spheroids and cylindrical rods. Eq 2 expresses the Stokes radius by a shape factor f_S (accounting for nonspherical shapes of the solute) and a correction factor c (accounting for the finite size of the solvent with respect to the solute).[6]

$$r_H = cf_S \tag{2}$$

In our case of small solvent molecules one can simply set $c = 1$.[78,79] The van der Waals radius of a THF molecule, for example, is about 0.3 nm which is smaller than any of the dye compounds.

However, the sizes of solvent molecules and dyes are in the same order of magnitude. One might assume that the solvent does not form a uniform environment of homogeneous (bulk) viscosity at the length scales of the molecules. These effects may cause deviations with respect to the ideal conditions that are assumed in the hydrodynamic models. Orientation-averaged form factors f_S have been determined for various shapes. The simplest deviations from a sphere are prolate and oblate spheroids. For these spheroids one finds[80−83]

$$\text{prolate}: \quad f_S = \frac{1}{2}\frac{a\sqrt{1-(b/a)^2}}{\ln\left[1+\sqrt{1-(b/a)^2}\right]-\ln(b/a)} \tag{3}$$

$$\text{oblate}: \quad f_S = \frac{1}{2}\frac{a\sqrt{(b/a)^2-1}}{\arctan\left[\sqrt{(b/a)^2-1}\right]} \tag{4}$$

where a and b represent the extensions of the spheroid along the symmetry axis and the two other axes, respectively ($b/a < 1$ for prolate and $b/a > 1$ for oblate spheroids).

The values for a and b in eqs 3 and 4 can be estimated from the molecular models. To do so, we first determined the principal axes of rotation Ψ, Θ, and Φ (in the order of the according moments of inertia). Finally, we projected all the atomic positions onto each principal axis and calculated the extension of the molecule along this direction. The values are listed in Table 3. The results suggest that compounds **3**, **7a**, **7b**, **7c**, and **8** appear as oblate spheroids (*i.e.*, the first axis is considerably shorter than the second and third) that become more spherical with increasing dendrimer generation due to the radial orientation and branching of the dendritic arms. However, compounds **5**, **6**, **9a** and **9b** look more like prolate spheroids. The structural dimensions of the dyes **1**, **2**, and **4** do not match the shape of a spheroid. In any case, the minimal fluorescence anisotropy of these compounds makes clear that the rotation of the molecules is so fast ($\tau_{rot} \ll 1$ ns) that all influences of the molecule's shape on the translational motion are averaged out. Hence, these small molecules appear as perfect spheres within the time scale of our measurements.

In addition to the deviations in shape, the solutes and solvents included in this study interact only weakly and have comparable molecular dimensions. For these conditions it is known that the obtained friction coefficients are systematically too large compared to experimental values. This discrepancy has been addressed by Zwanzig by changing the boundary conditions for solving the Navier−Stokes equation to obtain the friction coefficients.[84] Here, the tangential forces at the surface of the solute vanish allowing the solvent molecules to *slip* whereas in the classical treatment they *stick* on the surface of the solute. This approach correctly rendered the fast reorientation-times of molecules in organic solvents, which could not be explained otherwise.[85,86] But also the translation of molecules is faster under these *slip* conditions. Since the friction coefficients are systematically smaller, the corresponding Stokes-radius of the classical treatment appears to be too small. For a given shape of spheroidal rotors one can accordingly correct for this effect using the tabulated values in Zwanzig's paper.

Taking the above into account, we found the following values for the shape factors of the oblate structures: f_S = 0.9 nm (corresponding to 1.1 nm for *slip* boundary conditions) for **3**, f_S = 1.4 nm (2.0 nm) for **7a**, f_S = 1.7 nm (2.3 nm) for **7b**, f_S = 2.3 nm (3.3 nm) for **7c**, and f_S = 1.1 nm (1.5 nm) for **8**. Similarly, for the prolate structures we obtained f_S = 0.7 nm (0.9 nm) for **5**, f_S = 0.9 nm (1.2 nm) for **6**, f_S = 2.9 nm (4.3 nm) for **9a**, and f_S = 5.4 nm (8.1 nm) for **9b**.

These numbers show that it is difficult to account for all the subtle details that determine the diffusive behavior of molecules. If the structure is rigid and well-known (compounds **1**−**4**) the predictions of the modeling agree well to the experimental results. For molecules having flexible side groups (compounds **5**, **6**, and **8**) all models predict a radius larger than the experimental value. In situations where the *slip* boundary condition is justified, one could think of neglecting these groups for the determination of the spheroid dimensions. For the larger molecules (**7a**, **7b**, **7c**, **9a** and **9b**), whose structures are not determined to the required precision, the results are not conclusive and reasons for the observed trends remain speculative. The results indicate that one can more accurately describe the diffusion properties of a molecule using the shape factors, rather than by the simple approximation of a hard sphere. However, this approach still requires a sufficiently accurate structural model for the compound. For the large molecules in our series the available structures do not reach the required precision. A systematic study of all the structural effects on the hydrodynamic properties of molecules is clearly beyond the scope of this report. Its excellent performance renders 2fFCS a powerful tool for such investigations.

CONCLUSIONS

By means of recently developed dual-focus fluorescence correlation spectroscopy (2fFCS), we accurately and precisely determined absolute values for the translational diffusion constants of several dyes in a range of organic solvents. The selected dyes and organic solvents span the visible spectrum and a broad range of refractive indices, respectively. The diffusion constant values can be used as absolute reference standards for the calibration of experimental FCS setups. This does not limit the use of 1fFCS with organic media to relative measurements anymore and allows quantitative measurements to be performed. However, one should still try to minimize all possible sources of error in classical FCS, such as refractive index mismatch and optical saturation of the chromophores. We showed that a very limited set of commercially available, inexpensive fluorescent dyes can be easily dissolved and used in different solvents, thus ensuring rapid calibration of 1fFCS setups with different laser excitation lines and different sample environments, without the need for additional instrumentation or multiple measurements. The 2fFCS data for one of the blue-absorbing dyes in all four organic solvents were confirmed by pulsed-field gradient nuclear magnetic resonance spectroscopy experiments. Interestingly, in nearly all cases a particular dye shows similar Stokes radii in different organic solvents (including the polar solvent ethanol that can participate in hydrogen bonding), although the Stokes radius is, in principle, not only dependent on macroscopic viscosity, but also on specific microscopic interactions. We also showed that the obtained diffusion constants provide reliable information about the hydrodynamic dimensions of the fluorescent solutes, if a correct expression is used for the calculation of the Stokes radii.

METHODS

Chemicals. *Organic Solvents.* Four different organic solvents were selected on the basis of the following criteria: (i) commercial availability of spectrophotometric purity grade; (ii) widespread use in different fields of application; (iii) ability to dissolve a broad range of solutes (including many polymers); (iv) broad range of polarity; (v) relatively low vapor pressure to minimize solvent evaporation during the FCS measurements (nevertheless, a sealed sample holder should be used when working with volatile organic solvents); and (vi) most importantly, broad range of refractive indices. The refractive index of the sample is a key parameter, because it strongly influences the size and shape of the confocal volume element in FCS measurements. In combination with water, the selected solvents (ethanol, chloroform, THF, and toluene) cover a range of refractive indices between n_D = 1.33 and n_D = 1.50 (Table S2 in Supporting Information). This range comprises nearly all common organic solvents (Table S2),[74] as well as common polymers,[87,88] *e.g.*, poly(dimethylsiloxane) (PDMS): $n_D \approx 1.42$; poly(propylene oxide) (PPO): $n_D \approx 1.46$; poly(propylene) (PP): $n_D \approx 1.47$; poly(methyl methacrylate) (PMMA): $n_D \approx 1.49$; poly(isoprene) (PI): $n_D \approx 1.52$; poly(norbornene) (Zeonex): n_D = 1.50 to 1.55.

Organic solvents were purchased from Sigma-Aldrich (chloroform: spectrophotometric grade, >99.8% (stabilized with 0.5% to 1.0% EtOH); tetrahydrofuran (THF): spectrophotometric grade, >99.5%, free of stabilizers), Acros Organics (toluene: spectrophotometric grade, >99.0%, free of stabilizers), and Merck (ethanol: spectrophotometric grade (Uvasol), >99.9%, free of stabilizers), and were used as received after confirming their spectroscopic purity (i) by evaluating the detector photon count rate generated by the pure solvent in a FCS measurement and (ii) by visual inspection by means of single-molecule wide-field imaging of a cleaned cover slide after evaporation of a droplet of solvent.

Organosoluble Reference Dyes. The reference dyes were selected on the basis of the following criteria: (i) commercial availability of high-purity samples at a reasonable price; (ii) desirable photophysical properties such as a high molar extinction coefficient at common FCS laser line wavelengths (for example 470, 488, 514, 531, 543, 633, or 647 nm), a high fluorescence quantum yield, high photostability and a low yield of dark states (triplet state, electron transfer, *cis*−*trans* isomerization, *etc.*);[89] (iii) broad range of excitation wavelengths, allowing for calibration of a wide range of FCS setups equipped with different laser excitation lines covering almost the entire visible spectrum; (iv) chemical and thermal stability; (v) solubility and lack of tendency to aggregate in a broad range of common organic solvents.

TABLE 4. Selected Commercially Available Organosoluble Reference Dyes[a]

dye	CAS number	trivial name or abbreviation	supplier	purity (%)
1	155306−73−3	—	FEW Chemicals GmbH product S 2105	99.6
2	203381−28−6	—	FEW Chemicals GmbH product S 2112	99.8
3	331861−93−9	PDI G0ken/octyl-PTCDI	Organica Feinchemie GmbH product 59600	99.2
4	53340−16−2	Nile Blue A perchlorate	Acros Organics product 415705000	>99
5	127274−91−3	DiD/DiIC$_{18}$(5) oil	Life Technologies Europe B.V. product D-307	>99

[a] Purity of the sample was verified by ^{1}H NMR spectroscopy and HPLC analysis.

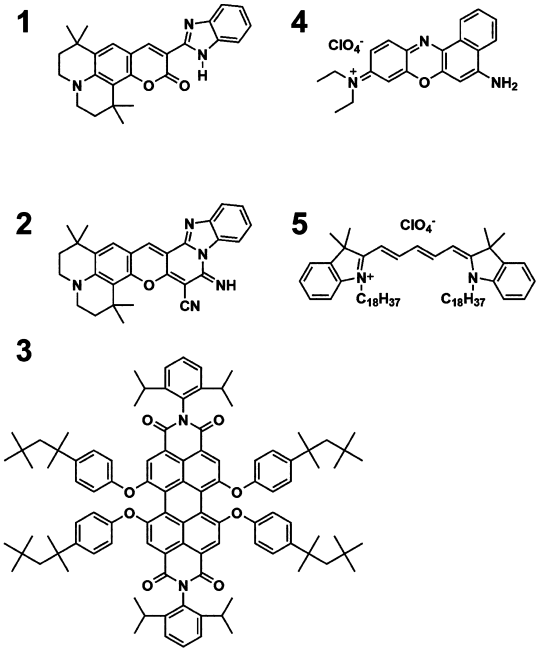

Scheme 1. Chemical structures of commercially available organosoluble reference dyes.

Thus, compounds **1**, **2**, **3**, **4** and **5** (Table 4 and Scheme 1) were acquired from FEW Chemicals GmbH (Bitterfeld-Wolfen, Germany), Organica Feinchemie GmbH (Bitterfeld-Wolfen, Germany), Life Technologies Europe (Ghent, Belgium) and Acros Organics (Geel, Belgium). Table S1 lists some photophysical properties of these chromophores.

In addition, rylene dyes **6**, **7a**−**7c** and **8** and the multichromophoric dendrimers **9a** and **9b** (Table 5 and Scheme 2) were investigated. The perylenediimide (PDI) and terrylenediimide (TDI) chromophores show excellent photophysical properties and photostability, and are widely used in single-molecule spectroscopy and microscopy research.[89] These compounds were synthesized by the Müllen group at the Max Planck Institute for Polymer Research (Mainz, Germany).

The chemical and spectroscopic purity of the dyes was confirmed *via* a certificate of analysis provided by the supplier, by ^{1}H NMR spectroscopy, and in case of **1**, **2**, **4**, and **5** also by means of high-pressure liquid chromatography (HPLC). Separation *via* HPLC (Agilent 1100, Agilent Technologies Belgium S.A., Diegem, Belgium) was done using a reverse-phase C_{18} column (Grace Prevail C_{18}, 150 mm × 2 mm, 3 μm particle size). After detection by a UV−vis DAD detector the fractions were analyzed by a single-quadrupole MS detector (Agilent 6110) using positive electrospray ionization. UV−vis detection was performed at 215 nm, at the laser excitation wavelength used for the investigated dye (either λ_{ex} = 470 nm, λ_{ex} = 531 nm, or λ_{ex} = 635 nm), and at the wavelength of maximal absorption. Thin layer chromatography (TLC) was used to check the purity of **3**, **6**, **7a**−**7c**, **8**, and **9a**−**9b**.

Finally, the purity of the chromophores and the lack of aggregate formation could be confirmed by the possibility to fit the ACFs with a single diffusion constant and by visual inspection of the photon count time traces.

TABLE 5. Selected Organosoluble Reference Dyes Provided by the Group of K. Müllen[a]

dye	description	abbreviation
6	swallow-tailed perylenediimide	PDI sw-C_7
7a	first-gen. perylenediimide polyphenylene dendrimer	PDI G1
7b	second-gen. perylenediimide polyphenylene dendrimer	PDI G2
7c	third-gen. perylenediimide polyphenylene dendrimer	PDI G3
8	first-gen. terrylenediimide polyphenylene dendrimer	TDI G1
9a	first-gen. multichromophoric perylenediimide dendrimer	multi-PDI(8)
9b	second-gen. multichromophoric perylenediimide dendrimer	multi-PDI(24)

[a] Purity of all samples was >99% as determined by ^{1}H NMR spectroscopy and MALDI-TOF mass spectrometry.

Sample Preparation. Samples were prepared by making dilutions of the dyes in a particular solvent (ethanol, chloroform, THF, or toluene) up to a concentration of about 1 nM (corresponding to about one or a few dye molecules on average inside one confocal volume element). The sample solutions in chloroform, THF or toluene were transferred to homemade, closed sample holders made of glass with a cleaned microscopy glass slide (#1.5 coverslips, Gerhard Menzel, Braunschweig, Germany) at the bottom (300 μL sample volume). Sample solutions in ethanol were measured in a chamber system with a #1.0 glass slide at the bottom (Nunc Lab-Tek II, Thermo Fisher Scientific, Braunschweig, Germany) and equipped with a cover to prevent solvent evaporation during the measurements. All glassware (vials for dilutions, sample holders, glass slides, pasteur pipettes, *etc.*) was thoroughly cleaned before use, by sonication in acetone (Sigma-Aldrich, spectrophotometric grade, >99.5%), sonication in aqueous NaOH (1 M) (twice) and sonication in milli-Q water (twice). In between the cleaning steps, the glassware was rinsed with milli-Q water. Finally, after drying under a flow of argon, it was kept in a UV−ozone photoreactor (PR-100, Ultraviolet Products, USA) for 3 h. This cleaning procedure rendered the glassware hydrophilic, thus reducing adhesion of hydrophobic dye molecules onto the surfaces.

Steady-State and Time-Resolved Spectroscopic Measurements. Steady-state absorption spectra were acquired using a UV−vis spectrophotometer (Lambda 40, PerkinElmer, Zaventem, Belgium). The optical density at the absorption maximum of all solutions was kept below A < 0.1 in a 1 cm quartz cuvette. Steady-state fluorescence emission spectra were recorded at room temperature (20.0 to 21.0 °C) using a fluorimeter (Fluorolog 3−22, HORIBA Jobin-Yvon, Lier, Belgium), corrected for the wavelength dependence of the detection system. Fluorescence decay times were determined from the TCSPC data that were acquired during the 2fFCS measurements (see below).

pfgNMR Measurements. We measured NMR spectra of **1** and **3** in $CDCl_3$, toluene-d_8, and THF-d_8 and of **1** and **2** in ethanol-d_6. Concentrations of all samples were 1.0 mM. Measurements were done with a 600 MHz spectrometer (INOVA, Varian) operating at the ^{1}H frequency of 599.644 MHz using a room temperature 3 mm probe head equipped with three orthogonal gradient coils. Self-diffusion constant measurements were performed applying the BPP-LED sequence.[90−96] The DOSY spectra

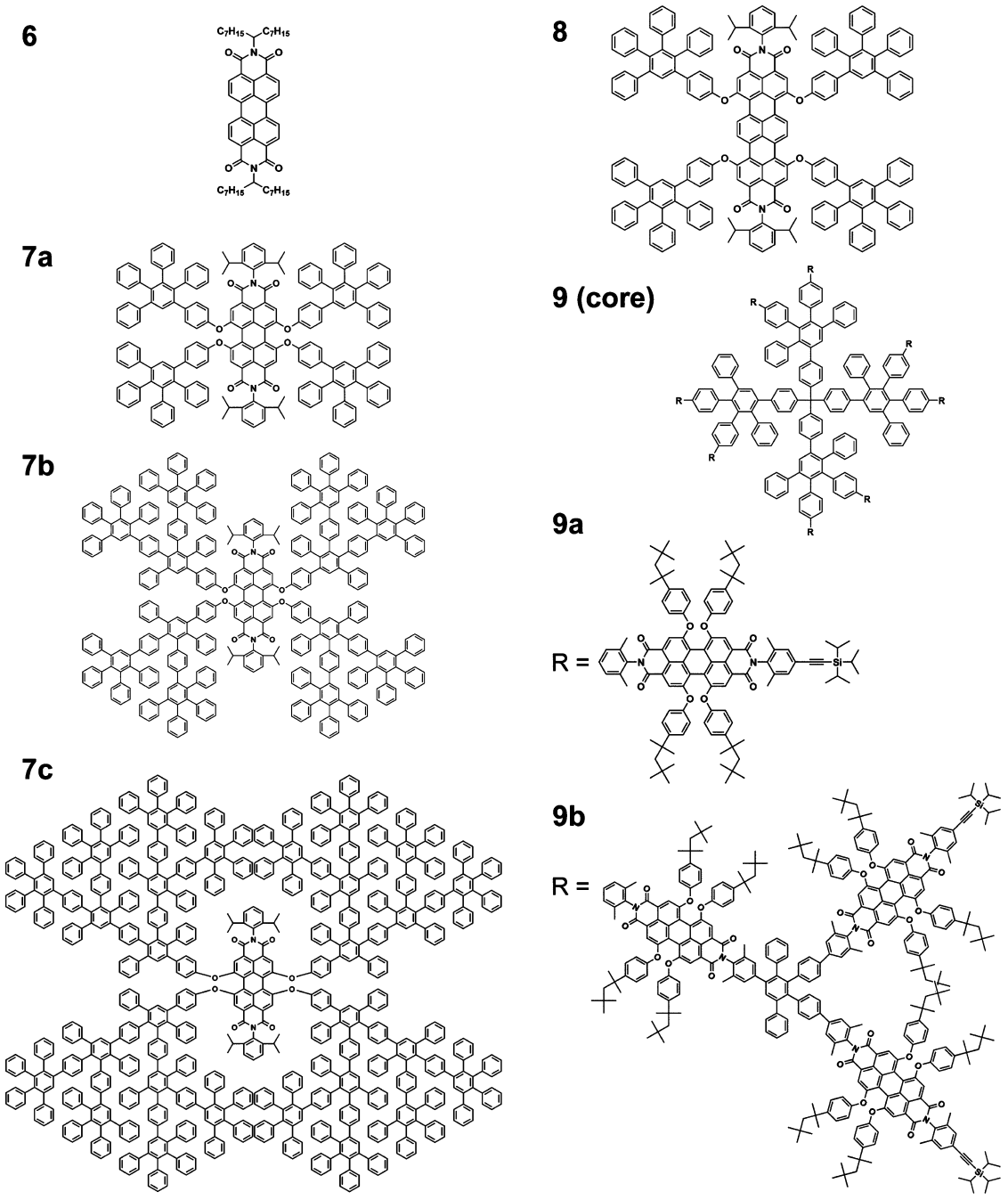

Scheme 2. Chemical structures of organosoluble reference dyes provided by the group of K. Müllen.

were acquired at 25 °C using a thermostat (L900, Varian) with temperature accuracy better than ±0.05%. The data were collected with no spinning. The self-diffusion constants were obtained in the following way. We calibrated our gradient using the D_T values previously obtained by NMR at 25 °C with a methanol-d_4 sample, namely for CD_3OH (D_T = 2220 $\mu m^2 s^{-1}$) and for CHD_2OD (D_T = 2180 $\mu m^2 s^{-1}$).[97] The gradient strength was logarithmically incremented in 15 steps from 145.2 mT m^{-1} up to 562.2 mT m^{-1}. In addition, we measured the self-diffusion constants of all (undeuterated) solvents as a reference: $CHCl_3$ in $CDCl_3$ (D_T = 2049 $\mu m^2 s^{-1}$), toluene in toluene-d_8 (D_T = 1910 $\mu m^2 s^{-1}$), THF in THF-d_8 (D_T = 2241 $\mu m^2 s^{-1}$), ethanol in ethanol-d_6 (D_T = 998 $\mu m^2 s^{-1}$).[98] The diffusion constants of TMS (D_T = 1760 $\mu m^2 s^{-1}$) as well as residual water (D_T = 4347 $\mu m^2 s^{-1}$) in $CDCl_3$ were also confirmed.[98] The following experimental settings were used: diffusion time was 40 ms, gradient duration was 800 ms, the longitudinal eddy current delay was 20 ms, and acquisition time was 3 s. Details of the apparatus and procedure are given elsewhere.[99−102] The reported self-diffusion constants are averages over at least ten measurements which agree to within ±0.5% and the overall accuracy of the data is estimated to be better than ±3.5%.

2fFCS Measurement Setups. Two different experimental setups were used. For the experiments with λ_{ex} = 470 nm or λ_{ex} = 635 nm laser light excitation, a commercial instrument was used (MicroTime 200, PicoQuant, Berlin, Germany). The instrument is based on an inverted epi-fluorescence microscope (IX-71, Olympus Europe, Hamburg, Germany). Excitation sources were two identical pulsed 470 nm diode lasers (LDH-P-C-470 B, PicoQuant) or two identical pulsed 635 nm diode lasers (LDH-P-635, PicoQuant) with linear polarization and a pulse duration of 50 ps (FWHM), respectively. The lasers were pulsed alternately

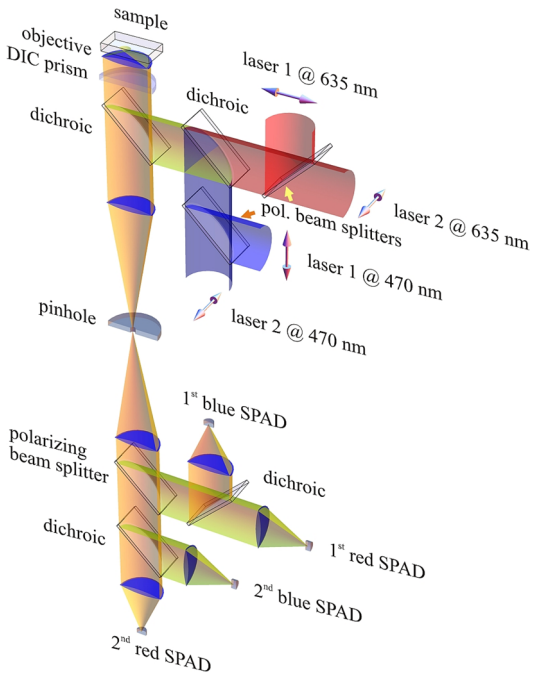

Figure 2. Schematic representation of the 2fFCS experimental setup for 470 nm and 635 nm excitation.

with a delay of 25 ns between pulses (PDL 828 Sepia II, PicoQuant). The light of each of the two pairs of identical wavelength but crossed polarization lasers was combined into single beams by two polarizing beam splitters (Ealing Catalogue, St. Asaph, United Kingdom). These beams were combined by a dichroic mirror (490dcxr, Chroma Technology Corp., Rockingham, VT, USA) into one single beam. Only one wavelength at a time was used for the 2fFCS measurements. A schematic illustration of the setup is shown in Figure 2.

An average power of 5 or 10 μW for each polarization was used. The beam was coupled into a polarization-preserving single-mode fiber. At the fiber output, the light was collimated (diameter ($1/e^2$) *ca.* 3 mm) and reflected toward the objective by a dichroic mirror (FITC/TRITC, Chroma). Before entering the back aperture of the objective, the light was passed through a Nomarski prism (U-DICTHC, Olympus) deflecting it into slightly different directions according to the polarization of the pulse. The light was focused by the microscope's water-immersion objective (UPLSAPO 60× W, 1.2 N.A., Olympus), creating two laterally shifted but overlapping excitation foci with about δ = 390 nm center distance in the case of λ_{ex} = 470 nm excitation, and with about δ = 450 nm center distance in the case of λ_{ex} = 635 nm excitation. The centers of the two foci were positioned about 30 μm above the glass slide surface. Fluorescence was collected by the same objective, passed through the dichroic mirror (thus being separated from the excitation light), and focused by a tube lens through a single circular aperture (ø = 150 μm). After the pinhole, the light was recollimated, split by a polarizing beam splitter cube (Ealing) and then again by two dichroic mirrors (640dcxr, Chroma), and refocused onto two pairs of SPADs. One pair was used for the detection of fluorescence showing a wavelength lower than λ_{em} < 640 nm (PDM 50-C, Micro Photon Devices, Milan, Italy), and the second pair was used to detect the far red emission (SPCM-AQR-13, PerkinElmer, Wellesley, MA, USA). Emission bandpass filters HC520/35 and HC692/40, respectively (Semrock Inc., Rochester, NY, USA), positioned directly in front of each detector, were used for blocking scattered light. Time-correlated single-photon counting (TCSPC) electronics (HydraHarp 400, PicoQuant) recorded the detected photons of all detectors independently with an absolute temporal resolution of 4 ps on a common time frame. Recording photon arrival times with ps time resolution allows associating each fluorescence photon to its corresponding excitation pulse and focus. With this information the autocorrelation function for each focus separately and the cross-correlation function between the foci can be calculated.

For measurements with λ_{ex} = 531 nm a second instrument was used being mostly identical to the one described above. The differences were as follows: For excitation the nonpolarized light of a supercontinuum laser (SC400−2-PP, Fianium Ltd., Southampton, United Kingdom; repetition rate 20 MHz) was divided by a polarizing beamsplitter (CM1-PBS251, Thorlabs, Dachau, Germany) into two linearly polarized beams. The beams were spectrally filtered using an acousto-optical tunable filter (AOTFnC-400.650, AAoptic S.A., Orsay Cedex, France) for each beam. The light of the first branch was delayed by 25 ns (*i.e.*, half the laser repetition period) using a polarization-preserving optical fiber of appropriate length (PMC-400Si, Schäfter und Kirchoff GmbH, Hamburg, Germany). A second polarizing beam splitter (CM1-PBS251, Thorlabs) was used to combine both beams before coupling them into a second identical polarization-preserving single-mode fiber. At the fiber output, the light formed a train of pulses (FWHM <10 ps) showing alternating polarization and a temporal spacing of 25 ns. An average power of 50 μW for each polarization was chosen. For detection the emission was split by a polarizing beamsplitter cube (CM1-PBS251, Thorlabs), and refocused onto two SPADs (τ-SPAD-50, PicoQuant). Emission long-pass filters HQ545LP (Chroma) were positioned directly in front of each detector.

Each dye/solvent combination was measured at least three times, and during each measurement fluorescence was collected for at least 15 min. The photon count time traces and correlation functions were inspected for the absence of potential distortions caused by photobleaching or passage of large aggregates through the confocal volume. Reported errors of the diffusion constant values in Table 1 are standard deviations derived from all measurements on a particular sample.

Data Analysis. When doing 2fFCS, it is important to use a model for the MDF that is more accurate than the usual assumption of a three-dimensional Gaussian distribution. We showed that the MDF can be satisfactorily approximated by a combination of a Gauss-Lorentz excitation intensity profile and a simple pinhole function.[4,20] Using this MDF $U(\vec{r})$ as a function of position $\vec{r}$ eq 5, the diffusion-related model CCF is given by eq 6, which has to be evaluated numerically.

$$U(x,y,z) = \frac{\kappa(z)}{\omega^2(z)}\exp\left[-\frac{2(x^2+y^2)}{\omega^2(z)}\right] \quad \text{with}$$

$$\kappa(z) = 1-\exp\left[-\frac{2a^2}{R_0^2+\left(\frac{\lambda_{em}z}{\pi n R_0}\right)^2}\right] \quad \text{and} \qquad (5)$$

$$\omega^2(z) = \omega_0^2+\left(\frac{\lambda_{ex}z}{\pi n\omega_0}\right)^2$$

where x, y and z are Cartesian coordinates with the z axis along the optical axis, a is the radius of the confocal pinhole, λ_{ex} is the excitation wavelength, λ_{em} is the center emission wavelength, and n is the sample refractive index. R_0 and ω_0 are free fit parameters describing the Rayleigh length and the minimal beam waist, respectively.

$$g_{12}(\tau) = g_\infty + 2\epsilon_1\epsilon_2 c\sqrt{\frac{\pi}{\Theta}}\int_\infty^\infty dz_1\int_\infty^\infty dz_2\,\frac{\kappa(z_1)\kappa(z_2)}{8\Theta+\omega^2(z_1)+\omega^2(z_2)}$$
$$\exp\left(-\frac{(z_2-z_1)^2}{4\Theta}-\frac{2\delta^2}{8\Theta+\omega^2(z_1)+\omega^2(z_2)}\right) \qquad (6)$$

where τ is the correlation lag-time and the abbreviation $\Theta = D_T\tau$ was used. The lateral distance between the two detection volumes (foci) is given by δ. The two factors ϵ_1 and ϵ_2 describe the overall detection efficiency in both detection volumes, respectively, and c is the concentration of the fluorescent molecules.

The model ACF of each focus is obtained by setting $\delta = 0$ and by replacing $\epsilon_1\ \epsilon_2$ by either ϵ_1^2 or ϵ_2^2, respectively, eq 7.

$$g_{nn}(\tau) = g_\infty + 2\epsilon_n^2 c\sqrt{\frac{\pi}{\Theta}}\int_\infty^\infty dz_1 \int_\infty^\infty dz_2 \frac{\kappa(z_1)\kappa(z_2)}{8\Theta + \omega^2(z_1) + \omega^2(z_2)} \exp\left(-\frac{(z_2 - z_1)^2}{4\Theta}\right) \tag{7}$$

If a dye shows fast photophysical relaxation (on the microsecond time scale), an additional exponential function should be added to the correlation functions in the usual way.[103] Thus, each set of two ACFs and two CCFs (forward and reverse CCF) is globally fitted, having as fit parameters ϵ_1, ϵ_2, c, R_0, ω_0, D_T, and—if necessary—a photophysical relaxation time. It should be noted that the diffusion constant D_T itself is a fit parameter, rather than the diffusion time τ_{diff} (*i.e.*, the time it takes for a fluorescent particle to cross the confocal volume element) in conventional FCS experiments. Analysis of the experimentally obtained 2fFCS data was performed with MatLab R2010b (The MathWorks GmbH, Ismaning, Germany) using a custom-made routine.[4,104]

Theoretical Estimation of Stokes Radii. The obtained Stokes radii of the dyes in the different solvents were compared with theoretically derived values. For this purpose, the molecular structures of compounds **1**−**6**, and **8** were optimized with the software package MOPAC2012[76] using the semiempirical PM7 Hamiltonian. The structures of **7a**−**7c**, **9a**, and **9b** were optimized using a molecular mechanics model (MM2 force field) as implemented in the software package Chem3D Ultra. We could have optimized the structure of **7a** using the PM7 Hamiltonian, also. In this case, however, we preferred to use the force-field optimization to be able to make comparisons to its larger analogues **7b** and **7c**. The Stokes radii of the optimized structures were estimated using the Hydropro10 software.[77] This approach has proven successful to model the hydrodynamics of molecules and particles of known geometry, see *e.g.*, refs 105, 106, and 107, and references therein.

Conflict of Interest: The authors declare no competing financial interest.

Acknowledgment. K.G. was a postdoctoral research fellow of the Research Foundation Flanders (FWO-Vlaanderen). Financial support from FWO-Vlaanderen and Deutsche Forschungsgemeinschaft (DFG, SFB755) is gratefully acknowledged. K.G. would like to thank the Enderlein group for pleasant stays in Göttingen; Daniel Jänsch and Dr. Chen Li (Max Planck Institute for Polymer Research, Mainz, Germany) for their kind gift of PDI dyes; Dr. Peter Dedecker (KU Leuven, Belgium) for stimulating discussions; and Bert Demarsin (KU Leuven, Belgium) for assistance with the HPLC measurements.

Supporting Information Available: UV−vis spectra, fluorescence emission spectra and photophysical properties of the investigated dyes are provided. The data also includes measured 2fFCS data, solvent properties, as well as PDB-files of the optimized structures. The Supporting Information is available free of charge on the ACS Publications website at DOI: 10.1021/acsnano.5b02371.

REFERENCES AND NOTES

1. Wöll, D.; Uji-i, H.; Schnitzler, T.; Hotta, J.-i.; Dedecker, P.; Herrmann, A.; De Schryver, F. C.; Müllen, K.; Hofkens, J. Radical Polymerization Tracked by Single Molecule Spectroscopy. *Angew. Chem., Int. Ed.* **2008**, *47*, 783–787.
2. Wöll, D.; Braeken, E.; Deres, A.; De Schryver, F. C.; Uji-i, H.; Hofkens, J. Polymers and Single Molecule Fluorescence Spectroscopy, What Can We Learn? *Chem. Soc. Rev.* **2009**, *38*, 313–328.
3. Wöll, D. Fluorescence Correlation Spectroscopy in Polymer Science. *RSC Adv.* **2014**, *4*, 2447–2465.
4. Dertinger, T.; Pacheco, V.; von der Hocht, I.; Hartmann, R.; Gregor, I.; Enderlein, J. Two-Focus Fluorescence Correlation Spectroscopy: A New Tool for Accurate and Absolute Diffusion Measurements. *ChemPhysChem* **2007**, *8*, 433–443.
5. Liu, W.; Cellmer, T.; Keerl, D.; Prausnitz, J. M.; Blanch, H. W. Interactions of Lysozyme in Guanidinium Chloride Solutions from Static and Dynamic Light-Scattering Measurements. *Biotechnol. Bioeng.* **2005**, *90*, 482–490.
6. Macchioni, A.; Ciancaleoni, G.; Zuccaccia, C.; Zuccaccia, D. Determining Accurate Molecular Sizes in Solution Through NMR Diffusion Spectroscopy. *Chem. Soc. Rev.* **2008**, *37*, 479–489.
7. Magde, D.; Elson, E. L.; Webb, W. W. Thermodynamic Fluctuations in a Reacting System - Measurement by Fluorescence Correlation Spectroscopy. *Phys. Rev. Lett.* **1972**, *29*, 705–708.
8. Elson, E. L.; Magde, D. Fluorescence Correlation Spectroscopy. I. Conceptual Basis and Theory. *Biopolymers* **1974**, *13*, 1–27.
9. Magde, D.; Elson, E. L.; Webb, W. W. Fluorescence Correlation Spectroscopy. II. An Experimental Realization. *Biopolymers* **1974**, *13*, 29–61.
10. Magde, D.; Webb, W. W.; Elson, E. L. Fluorescence Correlation Spectroscopy. III. Uniform Translation and Laminar Flow. *Biopolymers* **1978**, *17*, 361–376.
11. Enderlein, J.; Gregor, I.; Patra, D.; Fitter, J. Art and Artefacts of Fluorescence Correlation Spectroscopy. *Curr. Pharm. Biotechnol.* **2004**, *5*, 155–161.
12. Enderlein, J.; Gregor, I.; Patra, D.; Dertinger, T.; Kaupp, U. B. Performance of Fluorescence Correlation Spectroscopy for Measuring Diffusion and Concentration. *ChemPhysChem* **2005**, *6*, 2324–2336.
13. Rigler, R.; Mets, U.; Widengren, J.; Kask, P. Fluorescence Correlation Spectroscopy with High Count Rate and Low Background: Analysis of Translational Diffusion. *Eur. Biophys. J.* **1993**, *22*, 169–175.
14. Hess, S. T.; Webb, W. W. Focal Volume Optics and Experimental Artifacts in Confocal Fluorescence Correlation Spectroscopy. *Biophys. J.* **2002**, *83*, 2300–2317.
15. Perroud, T. D.; Huang, B.; Wallace, M. I.; Zare, R. N. Photon Counting Histogram for One-Photon Excitation. *ChemPhysChem* **2003**, *4*, 1121–1123.
16. Perroud, T. D.; Huang, B.; Wallace, M. I.; Zare, R. N. Photon Counting Histogram for One-Photon Excitation (Correction). *ChemPhysChem* **2003**, *4*, 1280.
17. Rigler, R.; Elson, E. S., Eds.; *Fluorescence Correlation Spectroscopy: Theory and Applications*; Springer: Berlin, 2001.
18. Müller, C. B.; Loman, A.; Pacheco, V.; Koberling, F.; Willbold, D.; Richtering, W.; Enderlein, J. Precise Measurement of Diffusion by Multi-Color Dual-Focus Fluorescence Correlation Spectroscopy. *Europhys. Lett.* **2008**, *83*, 46001.
19. Korlann, Y.; Dertinger, T.; Michalet, X.; Weiss, S.; Enderlein, J. Measuring Diffusion with Polarization-Modulation Dual-Focus Fluorescence Correlation Spectroscopy. *Opt. Express* **2008**, *16*, 14609–14616.
20. Loman, A.; Dertinger, T.; Koberling, F.; Enderlein, J. Comparison of Optical Saturation Effects in Conventional and Dual-Focus Fluorescence Correlation Spectroscopy. *Chem. Phys. Lett.* **2008**, *459*, 18–21.
21. Petrásek, Z.; Schwille, P. Precise Measurement of Diffusion Coefficients Using Scanning Fluorescence Correlation Spectroscopy. *Biophys. J.* **2008**, *94*, 1437–1448.
22. Gendron, P. O.; Avaltroni, F.; Wilkinson, K. J. Diffusion Coefficients of Several Rhodamine Derivatives as Determined by Pulsed Field Gradient-Nuclear Magnetic Resonance and Fluorescence Correlation Spectroscopy. *J. Fluoresc.* **2008**, *18*, 1093–1101.
23. Culbertson, C. T.; Jacobson, S. C.; Ramsey, J. M. Diffusion Coefficient Measurements in Microfluidic Devices. *Talanta* **2008**, *56*, 365–373.
24. Dertinger, T.; Loman, A.; Ewers, B.; Müller, C. B.; Krämer, B.; Enderlein, J. The Optics and Performance of Dual-Focus Fluorescence Correlation Spectroscopy. *Opt. Express* **2008**, *16*, 14353–14368.
25. Müller, C. B.; Loman, A.; Richtering, W.; Enderlein, J. Dual-Focus Fluorescence Correlation Spectroscopy of

Colloidal Solutions: Influence of Particle Size. *J. Phys. Chem. B* **2008**, *112*, 8236–8240.
26. Müller, C. B.; Weiß, K.; Richtering, W.; Loman, A.; Enderlein, J. Calibrating Differential Interference Contrast Microscopy with Dual-Focus Fluorescence Correlation Spectroscopy. *Opt. Express* **2008**, *16*, 155–161.
27. Müller, C. B.; Weiß, K.; Loman, A.; Enderlein, J.; Richtering, W. Remote Temperature Measurements in Femto-Liter Volumes Using Dual-Focus-Fluorescence Correlation Spectroscopy. *Lab Chip* **2009**, *9*, 1248–1253.
28. Müller, C. B.; Eckert, T.; Loman, A.; Enderlein, J.; Richtering, W. Dual-Focus Fluorescence Correlation Spectroscopy: A Robust Tool for Studying Molecular Crowding. *Soft Matter* **2009**, *5*, 1358–1366.
29. Weiß, K.; Enderlein, J. Lipid Diffusion within Black Lipid Membranes Measured with Dual-Focus Fluorescence Correlation Spectroscopy. *ChemPhysChem* **2012**, *13*, 990–1000.
30. Weiss, K.; Neef, A.; Van, Q.; Kramer, S.; Gregor, I.; Enderein, J. Quantifying the Diffusion of Membrane Proteins and Peptides in Black Lipid Membranes with 2-Focus Fluorescence Correlation Spectroscopy. *Biophys. J.* **2013**, *105*, 455–462.
31. Pieper, C.; Weiss, K.; Gregor, I.; Enderlein, J. In *Fluorescence Fluctuation Spectroscopy (FFS)*; Tetin, S. Y., Ed.; Elsevier: Amsterdam, 2013; Methods in Enzymology, Vol. 518; Chapter 8, pp 175−204.
32. Sengupta, A.; Pieper, C.; Enderlein, J.; Bahr, C.; Herminghaus, S. Flow of a Nematogen Past a Cylindrical Micro-Pillar. *Soft Matter* **2013**, *9*, 1937–1946.
33. Štefl, M.; Benda, A.; Gregor, I.; Hof, M. The Fast Polarization Modulation Based Dual-Focus Fluorescence Correlation Spectroscopy. *Opt. Express* **2014**, *22*, 885–899.
34. Müller, B. K.; Zaychikov, E.; Bräuchle, C.; Lamb, D. C. Pulsed Interleaved Excitation. *Biophys. J.* **2005**, *89*, 3508–3522.
35. Kapanidis, A. N.; Laurence, T. A.; Lee, N. K.; Margeat, E.; Kong, X.; Weiss, S. Alternating-Laser Excitation of Single Molecules. *Acc. Chem. Res.* **2005**, *38*, 523–533.
36. Tetin, S. Y.; Swift, K. M.; Matayoshi, E. D. Measuring Antibody Affinity and Performing Immunoassay at the Single Molecule Level. *Anal. Biochem.* **2002**, *307*, 84–91.
37. Kim, S. A.; Heinze, K. G.; Waxham, M. N.; Schwille, P. Intracellular Calmodulin Availability Accessed with Two-Photon Cross-Correlation. *Proc. Natl. Acad. Sci. U. S. A.* **2004**, *101*, 105–110.
38. Börsch, M.; Turina, P.; Eggeling, C.; Fries, J. R.; Seidel, C. A. M.; Labahn, A.; Gräber, P. Conformational Changes of the H^+-ATPase from Escherichia Coli upon Nucleotide Binding Detected by Single Molecule Fluorescence. *FEBS Lett.* **1998**, *437*, 251–254.
39. Sukhishvili, S. A.; Chen, Y.; Müller, J. D.; Gratton, E.; Schweizer, K. S.; Granick, S. Diffusion of a Polymer 'Pancake'. *Nature* **2000**, *406*, 146.
40. Sukhishvili, S. A.; Chen, Y.; Müller, J. D.; Gratton, E.; Schweizer, K. S.; Granick, S. Surface Diffusion of Poly-(Ethylene Glycol). *Macromolecules* **2002**, *35*, 1776–1784.
41. Granick, S.; Zhao, J.; Feng Xie, A.; Bae, S. C. Watching Macromolecules Diffuse at Surfaces and Under Confinement. *Macromol. Symp.* **2003**, *201*, 89–94.
42. Zhao, J.; Granick, S. A Tentative Route toward Nanofluidics: Directed Diffusion of Small Molecules Embedded within Adsorbed Polymers. *Macromolecules* **2003**, *36*, 5443–5446.
43. Mukhopadhyay, A.; Zhao, J.; Bae, S. C.; Granick, S. An Integrated Platform for Surface Forces Measurements and Fluorescence Correlation Spectroscopy. *Rev. Sci. Instrum.* **2003**, *74*, 3067–3072.
44. Zettl, H.; Häfner, W.; Böker, A.; Schmalz, H.; Lanzendörfer, M.; Müller, A. H. E.; Krausch, G. Fluorescence Correlation Spectroscopy of Single Dye-Labeled Polymers in Organic Solvents. *Macromolecules* **2004**, *37*, 1917–1920.
45. Best, A.; Pakula, T.; Fytas, G. Segmental Dynamics of Bulk Polymers Studied by Fluorescence Correlation Spectroscopy. *Macromolecules* **2005**, *38*, 4539–4541.
46. Liu, R.; Gao, X.; Adams, J.; Oppermann, W. A Fluorescence Correlation Spectroscopy Study on the Self-Diffusion of Polystyrene Chains in Dilute and Semidilute Solution. *Macromolecules* **2005**, *38*, 8845–8849.
47. Verheijen, W.; Hofkens, J.; Metten, B.; Vercammen, J.; Shukla, R.; Smet, M.; Dehaen, W.; Engelborghs, Y.; de Schryver, F. C. The Photo-Physical Properties of Dendrimers Containing 1,4-Dioxo-3,6-Diphenylpyrrolo[3,4-c]pyrrole (DPP) as a Core. *Macromol. Chem. Phys.* **2005**, *206*, 25–32.
48. Winkler, R. G.; Keller, S.; Rädler, J. O. Intramolecular Dynamics of Linear Macromolecules by Fluorescence Correlation Spectroscopy. *Phys. Rev. E* **2006**, *73*, 041919.
49. Koynov, K.; Mihov, G.; Mondeshki, M.; Moon, C.; Spiess, H. W.; Müllen, K.; Butt, H.-J.; Floudas, G. Diffusion and Conformation of Peptide-Functionalized Polyphenylene Dendrimers Studied by Fluorescence Correlation and ^{13}C NMR Spectroscopy. *Biomacromolecules* **2007**, *8*, 1745–1750.
50. Zettl, H.; Zettl, U.; Krausch, G.; Enderlein, J.; Ballauff, M. Direct Observation of Single Molecule Mobility in Semidilute Polymer Solutions. *Phys. Rev. E* **2007**, *75*, 061804.
51. Grabowski, C. A.; Mukhopadhyay, A. Diffusion of Polystyrene Chains and Fluorescent Dye Molecules in Semidilute and Concentrated Polymer Solutions. *Macromolecules* **2008**, *41*, 6191–6194.
52. Cherdhirankorn, T.; Best, A.; Koynov, K.; Peneva, K.; Müllen, K.; Fytas, G. Diffusion in Polymer Solutions Studied by Fluorescence Correlation Spectroscopy. *J. Phys. Chem. B* **2009**, *34*, 3355–3359.
53. Cherdhirankorn, T.; Harmandaris, V.; Juhari, A.; Voudouris, P.; Fytas, G.; Kremer, K.; Koynov, K. Fluorescence Correlation Spectroscopy Study of Molecular Probe Diffusion in Polymer Melts. *Macromolecules* **2009**, *42*, 4858–4866.
54. Cherdhirankorn, T.; Floudas, G.; Butt, H.-J.; Koynov, K. Effects of Chain Topology on the Tracer Diffusion in Star Polyisoprenes. *Macromolecules* **2009**, *42*, 9183–9189.
55. Modesti, G.; Zimmermann, B.; Börsch, M.; Herrmann, A.; Saalwächter, K. Diffusion in Model Networks as Studied by NMR and Fluorescence Correlation Spectroscopy. *Macromolecules* **2009**, *42*, 4681–4689.
56. Zettl, U.; Hoffmann, S. T.; Koberling, F.; Krausch, G.; Enderlein, J.; Harnau, L.; Ballauff, M. Self-Diffusion and Cooperative Diffusion in Semidilute Polymer Solutions As Measured by Fluorescence Correlation Spectroscopy. *Macromolecules* **2009**, *42*, 9537–9547.
57. Dorfschmid, M.; Müllen, K.; Zumbusch, A.; Wöll, D. Translational and Rotational Diffusion During Radical Bulk Polymerization: A Comparative Investigation by Full Correlation Fluorescence Correlation Spectroscopy (fcFCS). *Macromolecules* **2010**, *43*, 6174–6179.
58. Zettl, U.; Ballauff, M.; Harnau, L. A Fluorescence Correlation Spectroscopy Study of Macromolecular Tracer Diffusion in Polymer Solutions. *J. Phys.: Condens. Matter* **2010**, *22*, 494111.
59. Nguyen, T.-T.-T.; Türp, D.; Wang, D.; Nölscher, B.; Laquai, F.; Müllen, K. A Fluorescent, Shape-Persistent Dendritic Host with Photoswitchable Guest Encapsulation and Intramolecular Energy Transfer. *J. Am. Chem. Soc.* **2011**, *133*, 11194–11204.
60. Tsay, J. M.; Doose, S.; Weiss, S. Rotational and Translational Diffusion of Peptide-Coated CdSe/CdS/ZnS Nanorods Studied by Fluorescence Correlation Spectroscopy. *J. Am. Chem. Soc.* **2006**, *128*, 1639–1647.
61. Stempfle, B.; Dill, M.; Winterhalder, M. J.; Müllen, K.; Wöll, D. Single Molecule Diffusion and its Heterogeneity During the Bulk Radical Polymerization of Styrene and Methyl Methacrylate. *Polym. Chem.* **2012**, *3*, 2456–2463.
62. Koynov, K.; Butt, H.-J. Fluorescence Correlation Spectroscopy in Colloid and Interface Science. *Curr. Opin. Colloid Interface Sci.* **2012**, *17*, 377–387.
63. Doroshenko, M.; Gonzales, M.; Best, A.; Butt, H.-J.; Koynov, K.; Floudas, G. Monitoring the Dynamics of Phase Separation in a Polymer Blend by Confocal Imaging and Fluorescence Correlation Spectroscopy. *Macromol. Rapid Commun.* **2012**, *33*, 1568–1573.

64. Schaeffel, D.; Staff, R. H.; Butt, H.-J.; Landfester, K.; Crespy, D.; Koynov, K. Fluorescence Correlation Spectroscopy Directly Monitors Coalescence During Nanoparticle Preparation. *Nano Lett.* **2012**, *12*, 6012–6017.
65. Liu, D.; Wang, D.; Wang, M.; Zheng, Y.; Koynov, K.; Auernhammer, G. K.; Butt, H.-J.; Ikeda, T. Supramolecular Organogel Based on Crown Ether and Secondary Ammoniumion Functionalized Glycidyl Triazole Polymers. *Macromolecules* **2013**, *46*, 4617–4625.
66. Wang, D.; Yuan, Y.; Mardiyati, Y.; Bubeck, C.; Koynov, K. From Single Chains to Aggregates, How Conjugated Polymers Behave in Dilute Solutions. *Macromolecules* **2013**, *46*, 6217–6224.
67. Papadakis, C. M.; Košovan, P.; Richtering, W.; Wöll, D. Polymers in Focus: Fluorescence Correlation Spectroscopy. *Colloid Polym. Sci.* **2014**, *292*, 2399–2411.
68. Vagias, A.; Košovan, P.; Koynov, K.; Holm, C.; Butt, H.-J.; Fytas, G. Dynamics in Stimuli-Responsive Poly(*N*-isopropylacrylamide) Hydrogel Layers As Revealed by Fluorescence Correlation Spectroscopy. *Macromolecules* **2014**, *47*, 5303–5312.
69. Schaeffel, D.; Kreyes, A.; Zhao, Y.; Landfester, K.; Butt, H.-J.; Crespy, D.; Koynov, K. Molecular Exchange Kinetics of Diblock Copolymer Micelles Monitored by Fluorescence Correlation Spectroscopy. *ACS Macro Lett.* **2014**, *3*, 428–432.
70. Enderlein, J. Polymer Dynamics, Fluorescence Correlation Spectroscopy, and the Limits of Optical Resolution. *Phys. Rev. Lett.* **2012**, *108*, 108101.
71. Wohlfarth, C. In *Viscosity of Pure Organic Liquids and Binary Liquid Mixtures*; Lechner, M. D., Ed.; Springer: Berlin, 2009; Landolt−Börnstein: Numerical Data and Functional Relationships in Science and Technology—New Series. Group IV (Physical Chemistry), Vol. 25.
72. Wohlfarth, C.; Wohlfarth, B. In *Viscosity of Pure Organic Liquids and Binary Liquid Mixtures—Pure Organometallic and Organononmetallic Liquids, Binary Liquid Mixtures*; Lechner, M. D., Ed.; Springer: Berlin, 2001; Landolt−Börnstein's New Series Group IV (Physical Chemistry), Vol. 18A.
73. Wohlfarth, C.; Wohlfarth, B. In *Viscosity of Pure Organic Liquids and Binary Liquid Mixtures—Pure Organic Liquids*; Lechner, M. D., Ed.; Springer: Berlin, 2002; Landolt−Börnstein's New Series Group IV (Physical Chemistry), Vol. 18B.
74. Lide, D. R., Jr., Ed.; *CRC Handbook of Chemistry and Physics*, 89th ed.; CRC Press/Taylor and Francis: Boca Raton, FL, 2009.
75. Qu, J.; Zhang, J.; Grimsdale, A. C.; Müllen, K.; Jaiser, F.; Yang, X.; Neher, D. Dendronized Perylene Diimide Emitters: Synthesis, Luminescence, and Electron and Energy Transfer Studies. *Macromolecules* **2004**, *37*, 8297–8306.
76. Stewart, J. J. P. Optimization of Parameters for Semiempirical Methods I. Method. *J. Comput. Chem.* **1989**, *10*, 209–220.
77. Ortega, A.; Amoros, D.; García de la Torre, J. Prediction of Hydrodynamic and Other Solution Properties of Rigid Proteins from Atomic and Residue-Level Models. *Biophys. J.* **2011**, *101*, 892–898.
78. Chen, H.-C.; Chen, S.-H. Diffusion of Crown Ethers in Alcohols. *J. Phys. Chem.* **1984**, *88*, 5118–5121.
79. Espinosa, P. J.; García de la Torre, J. Theoretical Prediction of Translational Diffusion Coefficients of Small Rigid Molecules from Their Molecular Geometry. *J. Phys. Chem.* **1987**, *91*, 3612–3616.
80. Perrin, F. Mouvement Brownien d'un Ellipsoide (II). Rotation Libre et Dépolarisation des Fluorescences. Translation et Diffusion de Molécules Ellipsoidales. *J. Phys. Radium* **1936**, *7*, 1–11.
81. Koenig, S. H. Brownian Motion of an Ellipsoid. A Correction to Perrin's Results. *Biopolymers* **1975**, *14*, 2421–2423.
82. Tirado, M. M.; García de la Torre, J. Translational Friction Coefficients of Rigid, Symmetric Top Macromolecules. Application to Circular Cylinders. *J. Chem. Phys.* **1979**, *71*, 2581–2587.
83. Tirado, M. M.; Martínez, C. L.; García de la Torre, J. Comparison of Theories for the Translational and Rotational Diffusion Coefficients of Rod-Like Macromolecules. Application to Short DNA Fragments. *J. Chem. Phys.* **1984**, *81*, 2047–2052.
84. Hu, C.-M.; Zwanzig, R. Rotational Friction Coefficients for Spheroids with the Slipping Boundary Condition. *J. Chem. Phys.* **1974**, *60*, 4354–4357.
85. Higashigaki, Y.; Wang, C. H. Rayleigh-Brillouin Scattering Studies of Liquid and Supercooled Liquid *o*-Terphenyl. *J. Chem. Phys.* **1981**, *74*, 3175–3184.
86. Fytas, G.; Wang, C. H. Studies of Siloxane Oligomers by Depolarized Rayleigh Scattering. *J. Am. Chem. Soc.* **1984**, *106*, 4392–4396.
87. Katritzky, A. R.; Sild, S.; Karelson, M. Correlation and Prediction of the Refractive Indices of Polymers by QSPR. *J. Chem. Inf. Model.* **1998**, *38*, 1171–1176.
88. Xu, J.; Chen, B.; Zhang, Q.; Guo, B. Prediction of Refractive Indices of Linear Polymers by a Four-Descriptor QSPR Model. *Polymer* **2004**, *45*, 8651–8659.
89. Weil, T.; Vosch, T.; Hofkens, J.; Peneva, K.; Müllen, K. The Rylene Colorant Family − Tailored Nanoemitters for Photonics Research and Applications. *Angew. Chem., Int. Ed.* **2010**, *49*, 9068–9093.
90. Karlicek, R. F.; Lowe, I. J. A Modified Pulsed Gradient Technique for Measuring Diffusion in the Presence of Large Background Gradients. *J. Magn. Reson.* **1980**, *37*, 75–91.
91. Chen, A.; Johnson, C. S., Jr.; Lin, M.; Shapiro, M. J. Chemical Exchange in Diffusion NMR Experiments. *J. Am. Chem. Soc.* **1998**, *120*, 9094–9095.
92. Cotts, R. M.; Hoch, M. J. R.; Sun, T.; Markert, J. T. Pulsed Field Gradient Stimulated Echo Methods for Improved NMR Diffusion Measurements in Heterogeneous Systems. *J. Magn. Reson.* **1989**, *83*, 252–266.
93. Fordham, E. J.; Gibbs, S. J.; Hall, L. D. Partially Restricted Diffusion in a Permeable Sandstone: Observations by Stimulated Echo pfg-NMR. *Magn. Reson. Imaging* **1994**, *12*, 279–284.
94. Wu, D.; Chen, A.; Johnson, C. S., Jr. An Improved Diffusion-Ordered Spectroscopy Experiment Incorporating Bipolar-Gradient Pulses. *J. Magn. Reson., Ser. A* **1995**, *115*, 260–264.
95. Gibbs, S. J.; Johnson, C. S., Jr. A pfg-NMR Experiment for Accurate Diffusion and Flow Studies in the Presence of Eddy Currents. *J. Magn. Reson.* **1991**, *93*, 395–402.
96. Morris, K. F.; Johnson, C. S., Jr. Diffusion-Ordered Two-Dimensional Nuclear Magnetic Resonance Spectroscopy. *J. Am. Chem. Soc.* **1992**, *114*, 3139–3141.
97. Weingärtner, H.; Holz, M.; Sacco, A.; Trotta, M. The Effect of Site-Specific Isotopic Substitutions on Transport Coefficients of Liquid Methanol. *J. Chem. Phys.* **1989**, *91*, 2568–2574.
98. Holz, M.; Mao, X.; Seiferling, D.; Sacco, A. Experimental Study of Dynamic Isotope Effects in Molecular Liquids: Detection of Translation-Rotation Coupling. *J. Chem. Phys.* **1996**, *104*, 669–679.
99. Holz, M.; Weingärtner, H. Calibration in Accurate Spin-Echo Self-Diffusion Measurements using ^{1}H and Less-Common Nuclei. *J. Magn. Reson.* **1991**, *92*, 115–125.
100. Price, W. S. Pulsed-Field Gradient Nuclear Magnetic Resonance as a Tool for Studying Translational Diffusion: Part II. Experimental Aspects. *Concepts Magn. Reson.* **1998**, *10*, 197–237.
101. Johnson, C. S., Jr. Diffusion Ordered Nuclear Magnetic Resonance Spectroscopy: Principles and Applications. *Prog. Nucl. Magn. Reson. Spectrosc.* **1999**, *34*, 203–256.
102. Antalek, B. Using Pulsed Gradient Spin Echo NMR for Chemical Mixture Analysis: How to Obtain Optimum Results. *Concepts Magn. Reson.* **2002**, *14*, 225–258.
103. Widengren, J.; Mets, U.; Rigler, R. Fluorescence Correlation Spectroscopy of Triplet States in Solution: A Theoretical and Experimental Study. *J. Phys. Chem.* **1995**, *99*, 13368–13379.

104. Wahl, M.; Gregor, I.; Patting, M.; Enderlein, J. Fast Calculation of Fluorescence Correlation Data with Asynchronous Time-Correlated Single-Photon Counting. *Opt. Express* **2003**, *11*, 3583–3591.
105. Hoffmann, M.; Wagner, C. S.; Harnau, L.; Wittemann, A. 3D Brownian Diffusion of Submicron-Sized Particle Clusters. *ACS Nano* **2009**, *3*, 3326–3334.
106. Carrasco, B.; García de la Torre, J. Hydrodynamic Properties of Rigid Particles: Comparison of Different Modeling and Computational Strategies. *Biophys. J.* **1999**, *76*, 3044–3057.
107. García de la Torre, J.; del Rio Echenique, G.; Ortega, A. Improved Calculation of Rotational Diffusion and Intrinsic Viscosity of Bead Models for Macromolecules and Nanoparticles. *J. Phys. Chem. B* **2007**, *111*, 955–961.
108. Triplet states can show a much longer lifetime in organic solvents than in aqueous solutions because the concentration of oxygen is usually quite small. Therefore, it is advisable to reduce the excitation power as much as possible.